

Intrinsic planar Hall effect in time-reversal-broken Weyl semimetals

Longjun Xiang¹ and Jian Wang^{1,2,*}

¹College of Physics and Optoelectronic Engineering, Shenzhen University, Guangdong, P. R. China

²Department of Physics, University of Hong Kong, Pokfulam Road, Hong Kong, P. R. China

The exotic responses of topological Weyl semimetals (WSMs) probed by electric (\mathbf{E}) and magnetic (\mathbf{B}) fields have been intensively explored recently. In this work, we predict that the intrinsic planar Hall effect (IPHE), in which the \mathbf{E} , \mathbf{B} , and the Hall current share the same plane, can emerge in time-reversal-broken WSMs. We reveal that the (field-induced) Berry curvature, arising from the nontrivial band geometry of the WSMs, is responsible for this effect, associated with the energy correction under \mathbf{E} and \mathbf{B} up to the second order. Importantly, dictated by the \mathbf{k} -space Lorentz force provided by this (field-induced) Berry curvature, the IPHE conductivity tensor features the anti-symmetric form, quite distinct from its extrinsic counterpart with a symmetric form reported in [Phys. Rev. Lett. 119, 176804 (2017)]. Particularly, employing a linearly tilted effective model, the dependence of the IPHE on the tilt direction and the angle formed by \mathbf{E} and \mathbf{B} are illuminated. Interestingly, by studying angular dependence, we find that the IPHE responses exist even when $\mathbf{E} \cdot \mathbf{B} = 0$, indicating that the Berry curvature plays a more fundamental role than the *chiral anomaly* in WSMs. Finally, the candidate materials to detect IPHE and the experimental strategy to distinguish the IPHE response of the WSMs from its extrinsic counterpart is discussed. Our work offers a novel intrinsic topological response function to detect magnetic WSMs and opens a new window to understanding the experimental results observed in magnetic WSMs.

Introduction — Capturing the intrinsic topological response of quantum matter is one of the most important themes in modern condensed matter physics¹. For example, the quantum Hall effect²⁻⁴, characterizing an intrinsic edge current response in time-reversal-broken (\mathcal{T} -broken) systems, initialized the concept of topology in modern condensed matter physics. Furthermore, the theoretical prediction⁵⁻⁷ and experimental observations⁸⁻¹⁰ of topological insulators, featuring the intrinsic dissipationless edge/surface current response, popularized the studies of the topological phase and topological classification¹¹⁻¹³ of quantum materials.

Recently, the topological phases of semimetal, such as the Dirac semimetals^{14,15} and Weyl semimetals (WSMs)¹⁶⁻¹⁸ protected by their nontrivial band topology, have attracted intensive research interest. Particularly, the WSMs, taking the massless Weyl fermions¹⁹ as its low-energy excitation, display a plethora of exotic response properties under electromagnetic fields, such as the Magnus response²⁰, the chiral magnetic effect (CME)²¹ and positive longitudinal magnetoconductance (LMC)²²⁻²⁴ induced by *chiral anomaly*²⁵⁻²⁹. Importantly, Nandy *et al.*³⁰ predicted that the PHE, also attributed to the *chiral anomaly* and the Berry curvature, can occur in type-I and type-II WSMs³¹, by solving the Boltzmann equation with the help of the first-order semiclassical theory³². Despite the great progress, the CME and PHE discussed until now are extrinsic (depends on the relaxation time τ) responses. In addition, to their physical origin, the relation between the *chiral anomaly* and the Berry curvature of WSMs is still vague.

In this *Letter*, the IPHE (free of τ and depends only on the band topology) at $EB/EB^2/E^2B/E^2B^2$ orders, as the topological response of \mathcal{T} -broken WSMs, is predicted with the semiclassical theory up to the second order. We unveil that the IPHE is engendered by the (field-induced) Berry curvature, which arises from the nontrivial band geometry of WSMs, and by the Bloch band energy corrected by electromagnetic fields up to the second order. Importantly, the \mathbf{k} -space Lorentz force, offered by this (field-induced) Berry curvature, dictates

that the IPHE conductivity be an anti-symmetric tensor, very different from its extrinsic counterpart with a symmetric form reported in Ref.[30]. Particularly, using a linearly tilted effective model, we study how the IPHE response depends on the tilt direction and extract the angular (the angle θ formed by \mathbf{E} and \mathbf{B}) dependence when the tilt direction is fixed. Interestingly, by analyzing the angular dependence of the IPHE, we find the IPHE response at different orders can exist even when the \mathbf{E} -field is perpendicular to the \mathbf{B} -field, namely when the *chiral anomaly* is missing, which indicates that the Berry curvature plays a more fundamental role than the *chiral anomaly* in WSMs. Finally, the candidate materials to detect IPHE and the experimental strategy to distinguish the IPHE response of the WSMs from its extrinsic counterpart is discussed. This work provides a novel intrinsic topological response function to detect magnetic WSMs and may facilitate understanding the experimental measurement performed in magnetic WSMs.

Semiclassical dynamics — The semiclassical equation of motion including the correction from electromagnetic fields (denoted as $\mathbf{E} \equiv E\hat{\mathbf{E}}$ and $\mathbf{B} \equiv B\hat{\mathbf{B}}$ with $\hat{\mathbf{E}}$ and $\hat{\mathbf{B}}$ the directional vector, respectively) for both the band energy and Berry curvature is given by³³ ($\hbar = e = 1$),

$$\begin{aligned}\dot{\mathbf{r}} &= -\dot{\mathbf{k}} \times \tilde{\boldsymbol{\Omega}} + \tilde{\mathbf{v}}_{\mathbf{k}} \\ \dot{\mathbf{k}} &= -\dot{\mathbf{r}} \times \mathbf{B} - \mathbf{E}\end{aligned}\quad (1)$$

where $\tilde{\mathbf{v}}_{\mathbf{k}} = \nabla_{\mathbf{k}} \tilde{\epsilon}(\mathbf{k})$ is the group velocity with $\tilde{\epsilon}(\mathbf{k})$ the band energy including the second-order correction of the external fields, and $\tilde{\boldsymbol{\Omega}} = \boldsymbol{\Omega} + \boldsymbol{\Omega}^{(1)}$ with $\boldsymbol{\Omega}$ the conventional Berry curvature³² and $\boldsymbol{\Omega}^{(1)}$ the first-order field-induced Berry curvature³³. Specifically,

$$\boldsymbol{\Omega}^{(1)} \equiv \boldsymbol{\Omega}^E E + \boldsymbol{\Omega}^B B \quad (2)$$

with $\boldsymbol{\Omega}^E E = \nabla_{\mathbf{k}} \times \mathcal{A}^{(1, B=0)}$ and $\boldsymbol{\Omega}^B B = \nabla_{\mathbf{k}} \times \mathcal{A}^{(1, E=0)}$, where $\mathcal{A}^{(1)}$ is the first-order *positional shift*³³ induced by \mathbf{E} and \mathbf{B} .

In Eq.(1), $\dot{\mathbf{r}} \times \mathbf{B}$ is the Lorentz force in real space while $\dot{\mathbf{k}} \times \tilde{\boldsymbol{\Omega}}$ can be viewed as the \mathbf{k} -space Lorentz force³². As an important consequence of this Lorentz force in \mathbf{k} -space, we find that the IPHE conductivity tensors feature the anti-symmetric form, completely different from its extrinsic counterpart, as will be illustrated later. Solving for $\dot{\mathbf{r}}$ and $\dot{\mathbf{k}}$ from Eq.(1), we have

$$\dot{\mathbf{r}} = D^{-1}[\tilde{\mathbf{v}}_{\mathbf{k}} + \mathbf{E} \times \tilde{\boldsymbol{\Omega}} + \mathbf{B}(\tilde{\mathbf{v}}_{\mathbf{k}} \cdot \tilde{\boldsymbol{\Omega}})] \quad (3a)$$

$$\dot{\mathbf{k}} = D^{-1}[-\mathbf{E} - \tilde{\mathbf{v}}_{\mathbf{k}} \times \mathbf{B} - \tilde{\boldsymbol{\Omega}}(\mathbf{E} \cdot \mathbf{B})] \quad (3b)$$

where $D = 1 + \mathbf{B} \cdot \tilde{\boldsymbol{\Omega}}$ is the phase space measurement. Furthermore, by substituting Eq.(3a) into the charge current density³² $\mathbf{J} \equiv \int_{\mathbf{k}} D \dot{\mathbf{f}} \dot{\mathbf{r}}$, we finally obtain³⁴

$$\mathbf{J} = \int_{\mathbf{k}} f_{\mathbf{k}}(\tilde{\epsilon}_{\mathbf{k}})[\tilde{\mathbf{v}}_{\mathbf{k}} + \mathbf{E} \times \tilde{\boldsymbol{\Omega}} + \mathbf{B}(\tilde{\mathbf{v}}_{\mathbf{k}} \cdot \tilde{\boldsymbol{\Omega}})] \quad (4)$$

where $\int_{\mathbf{k}} \equiv \int d\mathbf{k}/(2\pi)^d$ with d the spatial dimensionality and $\tilde{f}_{\mathbf{k}} = f_{\mathbf{k}}(\tilde{\epsilon}_{\mathbf{k}})$ is the nonequilibrium distribution function. It is easy to show that $\int_{\mathbf{k}} \tilde{f}_{\mathbf{k}} \tilde{\mathbf{v}}_{\mathbf{k}} = \int_{\mathbf{k}} f_{\mathbf{k}}(\epsilon_{\mathbf{k}}) \mathbf{v}_{\mathbf{k}}$ ³⁵ with $\epsilon_{\mathbf{k}}$ and $\mathbf{v}_{\mathbf{k}}$ the unperturbed band energy and group velocity, respectively. Therefore, in the following, we will focus on the second term of Eq.(4) to achieve the IPHE. The last term in Eq.(4), including LMC and PHE components can be studied similarly and will be discussed in Supplemental Material³⁵. In particular, we will consider the linearly tilted WSMs described by

$$H = C_{\chi} \mathbf{t} \cdot \mathbf{k} + \chi \mathbf{k} \cdot \boldsymbol{\sigma} \quad (5)$$

where $\chi = \pm 1$ is the chirality index, \mathbf{k} the crystal momentum, $\boldsymbol{\sigma}$ the vector of the Pauli matrices, $\mathbf{t} = (t_x, t_y, t_z)$ the tilt vector, and $C_{\chi} = a_1 + b_1 \chi$ with a_1/b_1 being 0 or 1. The presence of the tilt term breaks the \mathcal{T} -symmetry and hence ensures the achievement of IPHE. In addition, we note that $a_1 = 1$ further breaks the inversion symmetry (\mathcal{P})³⁶⁻⁴² and in the case of $a_1 = b_1 = 1$, it corresponds to a hybrid WSM with one Weyl point (WP) type I and the other one type II⁴³. In this work, Eq.(4) and Eq.(5) constitute the starting point to explore the IPHE response in \mathcal{T} -broken WSMs.

Chiral anomaly in WSMs — Before discussing the intrinsic current responses of tilted WSMs under \mathbf{E} and \mathbf{B} , it will be beneficial to illuminate the key concept of the *chiral anomaly* in WSMs and, more importantly, its relation with the Berry curvature, within the framework of semiclassical transport theory. Using the Boltzmann equation with the relaxation time approximation,

$$\partial_t \tilde{f}_{\mathbf{k}} + \dot{\mathbf{r}} \cdot \nabla_{\mathbf{r}} \tilde{f}_{\mathbf{k}} + \dot{\mathbf{k}} \cdot \nabla_{\mathbf{k}} \tilde{f}_{\mathbf{k}} = (\tilde{f}_{\mathbf{k}} - f_0)/\tau$$

along with charge density $\rho_{\chi} = \int_{\mathbf{k}} D \tilde{f}_{\mathbf{k}}$ and charge current density $\mathbf{J}_{\chi} = \int_{\mathbf{k}} D \tilde{f}_{\mathbf{k}} \dot{\mathbf{r}}$, it is easy to find

$$\partial_t \rho_{\chi} + \nabla \cdot \mathbf{J}_{\chi} + \int_{\mathbf{k}} D \dot{\mathbf{k}} \cdot \nabla_{\mathbf{k}} \tilde{f}_{\mathbf{k}} = \delta \rho_{\chi} / \tau. \quad (6)$$

Moreover, by performing integration by parts on the third term of Eq.(6) and using Eq.(3b) as well as $\nabla_{\mathbf{k}} \cdot \tilde{\boldsymbol{\Omega}} = \chi \delta(\mathbf{k})/2\pi$, which indicates that the Berry curvature of WSMs is

divergence-free except at WP with one monopole charge^{27,44}, we arrive at the modified continuity equation^{27,45,46}

$$\partial_t \rho_{\chi} + \nabla \cdot \mathbf{J}_{\chi} - \frac{\chi}{8\pi^3} \mathbf{E} \cdot \mathbf{B} = \delta \rho_{\chi} / \tau. \quad (7)$$

Clearly, when $\mathbf{E} \cdot \mathbf{B} \neq 0$ in Eq.(7), namely, the \mathbf{E} is not perpendicular to the \mathbf{B} , the monopole charge originated from the Berry curvature gives rise to a chirality-dependent chemical potential, which will make the current of Weyl fermions for each chirality non-conserving in the clean limit and hence was dubbed as the *chiral anomaly*. Therefore, we argue that the Berry curvature plays a more fundamental role than the *chiral anomaly* in WSMs, and this argument becomes clear when considering both the intrinsic and extrinsic PHE responses engendered by the (field-induced) Berry curvature and the energy correction for Bloch bands up to the second order.

Particularly, within the framework of the second-order semiclassical theory³³, both the (field-induced) Berry curvature and energy correction of the WSMs contains chirality-independent and chirality-dependent contributions. As a result, the combination of the (field-induced) Berry curvature and the energy correction will make the cancelation between different chiralities inactive. This will lead to two distinctive results illustrated below: (1). When $\mathbf{E} \cdot \mathbf{B} \neq 0$, the IPHE response driven by the (field-induced) Berry curvature from two WPs will not cancel with each other, indicating the Berry curvature or the *chiral anomaly* as the origin of IPHE in WSMs; (2). When the *chiral anomaly* is absent ($\mathbf{E} \cdot \mathbf{B} = 0$), the IPHE response still exists, showing that the Berry curvature plays a more fundamental role than the *chiral anomaly* in WSMs.

The IPHE — Next, we study how to achieve the IPHE response, that is free of the relaxation time τ , by using Eq.(4) and Eq.(5). Assuming $\hat{\mathbf{E}} = \hat{e}_x$ and $\hat{\mathbf{B}} = \cos \theta \hat{e}_x + \sin \theta \hat{e}_y$ with \hat{e}_{α} ($\alpha = x, y, z$) the basis vector, the IPHE current density obtained from the second term of Eq.(4) is written as

$$J_y = \sum_{\chi} \int_{\mathbf{k}} f_{\mathbf{k}} \tilde{\Omega}_z E, \quad (8)$$

where we have set $\tilde{f}_{\mathbf{k}} = f_{\mathbf{k}}$ with $f_{\mathbf{k}}$ the equilibrium Fermi distribution function but taking into account the energy correction from \mathbf{E} and \mathbf{B} . In addition, the summation over chirality χ in Eq.(8) is also shown explicitly. We emphasize that this term comes from \mathbf{k} -space Lorentz force $\mathbf{E} \times \tilde{\boldsymbol{\Omega}}$, which dictates that the IPHE conductivity tensor is anti-symmetric while keeping the $\hat{\mathbf{B}}$ unchanged, quite different from its extrinsic counterpart.

By expanding the equilibrium Fermi distribution function in terms of the first- and second-order energy corrections, we have

$$f_{\mathbf{k}} = f + f' [\epsilon^{(1)} + \epsilon^{(2)}] + \frac{1}{2} f'' [\epsilon^{(1)} + \epsilon^{(2)}]^2 \quad (9)$$

where $f' = \partial_{\epsilon} f$, $f'' = \partial_{\epsilon}^2 f$, $\epsilon^{(1)} = -\mathbf{B} \cdot \mathbf{m} \equiv \epsilon^B B$ the first-order energy correction with \mathbf{m} the orbital magnetic moment³², and $\epsilon^{(2)} \equiv \epsilon^{EE} E^2 + \epsilon^{EB} EB + \epsilon^{BB} B^2$ the second-order energy correction. Particularly, using Eq.(5), for the

lower band we find³⁵

$$\begin{aligned} \epsilon^B &= \chi \frac{k_x \cos \theta + k_y \sin \theta}{2k^2} & \epsilon^{EE} &= \frac{k_x^2 - k_y^2}{8k^5} \\ \epsilon^{EB} &= \frac{3k_z \sin \theta}{8k^4} & \epsilon^{BB} &= \lambda_0 + \lambda_1 C_\chi + \lambda_2 C_\chi^2 \end{aligned} \quad (10)$$

where $k^2 = k_x^2 + k_y^2 + k_z^2$ and the coefficients λ_i for ϵ^{BB} are listed in Supplemental Material³⁵. Note that ϵ^{EE} and ϵ^{EB} are chirality-independent, ϵ^B is chirality-dependent whereas ϵ^{BB} may include a chirality-dependent contribution. On the other hand, the Berry curvature $\tilde{\Omega}_z$ can be expressed as

$$\tilde{\Omega}_z \equiv \Omega_z + \Omega_z^E E + \Omega_z^B B \quad (11)$$

Also with Eq.(5), for the lower band we find³⁵

$$\begin{aligned} \Omega_z &= \chi \frac{k_z}{2k^3} & \Omega_z^E &= -\frac{k_y}{2k^5} \\ \Omega_z^B &= \left(C_\chi \frac{t_z}{2k^5} + \frac{k_z}{2k^6} \right) (k_x \cos \theta + k_y \sin \theta) \end{aligned} \quad (12)$$

where the conventional Berry curvature Ω_z is chirality-dependent, the E -induced Ω_z^E is chirality-independent and the B -induced Ω_z^B may also include a chirality-dependent contribution.

Furthermore, by combining the Eq.(9) with Eq.(11) and rewriting $J_y \equiv \sum_{l,m} \sigma_y^{(l,m)} E^l B^m$ with $\sigma_y^{(l,m)} \equiv \sum_\chi \int_k W^{(l,m)}$ the IPHE conductivity tensor (Here l/m be 1 or 2 because we are only interested in the terms up to the second order in E and B), we obtain the following integrands for the IPHE conductivity tensor:

$$W^{(1,1)} = f \Omega_z^B + f' \epsilon^B \Omega_z \quad (13a)$$

$$W^{(1,2)} = \chi f' \epsilon^{BB} \Omega_z + \chi f' \epsilon^B \Omega_z^B \quad (13b)$$

$$W^{(2,2)} = f' \epsilon^{EB} \Omega_z^B + f' \epsilon^{BB} \Omega_z^E + \frac{f''}{2} (\epsilon^B)^2 \Omega_z^E \quad (13c)$$

where the combinations, such as $W^{(2,1)}$, are forbidden by χ summation and the term $(\mathbf{E} \times \mathbf{\Omega})$ leading to the intrinsic anomalous Hall effect (IAHE) has been dropped. When the WSMs respect \mathcal{T} -symmetry, namely the tilted term in Eq.(5) is switched off, we find that the IPHE response contributed by Eq.(13) will be prohibited, same as the IAHE only supported by \mathcal{T} -broken systems. In addition, we note that all terms in Eq.(13) are Fermi surface property due to the presence of f' ^{32,47}.

Although the tilt term in Eq.(5) ensures the realization of IPHE response, we find $\sigma_y^{(l,m)}$ exhibits different behavior in the tilt direction and hence may feature different angular dependence on this tilt direction, which is the key to experimentally detecting the IPHE responses at different orders and to identify the relation between the Berry curvature and the *chiral anomaly*. For example, the dependence of $\sigma_y^{(1,1)}$ on tilt direction and on the θ formed by E and B , contributed by the first term of Eq.(13a), can be obtained as³⁵:

$$\sigma_y^{(1,1)} = \hat{t}_z (\hat{t}_x C_1 \cos \theta + \hat{t}_y C_2 \sin \theta) \quad (14)$$

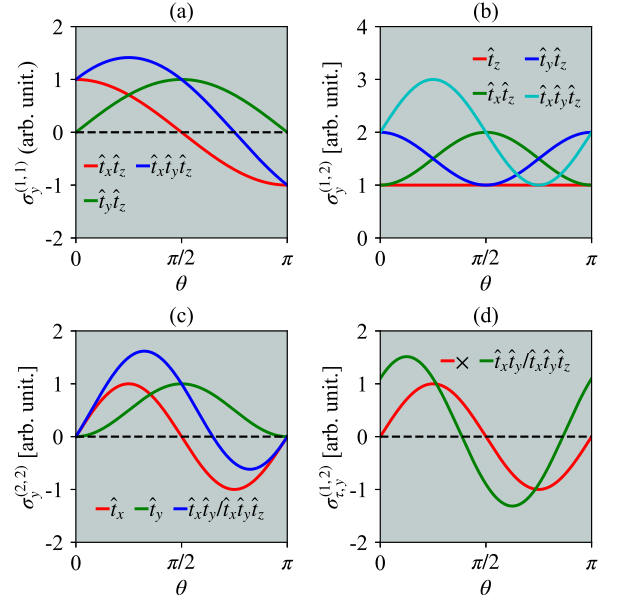


FIG. 1. (a-c) The dependence on tilt direction and the θ for IPHE conductivity tensors $\sigma_y^{(1,1)}$, $\sigma_y^{(1,2)}$, and $\sigma_y^{(2,2)}$, respectively. Here we are only interested in the tilt direction and angular dependence and hence set $C_i \equiv 1$ and $\hat{t}_\alpha \equiv 1$ in Eqs. (14-16). In (a) and (b), if $t_z = 0$ no linear IPHE response. In (c), the nonlinear IPHE is independent of t_z . (d) The tilt and angular dependence for extrinsic PHE at the order of EB^2 . Here we have set $C_1 = C_2 = 1$ and $C_3 = 0.1$ in Eq.(17), in which a tilt-free (denoted as \times) term is obtained.

where C_i stands for the Fermi-surface-dependent constants, which decides the magnitude of the IPHE response and will be estimated later, and \hat{t}_α with $\alpha = x, y, z$ are the tilt indicators to explicitly show the existence of C_i (This convention also will be adopted hereafter). In terms of Eq.(14), it is easily found that the tilt vector \mathbf{t} must have a nonzero projection on the t_x - t_y - t_z plane to capture a nonvanishing IPHE response at EB order. In FIG.(1a), we show the angular dependence of $\sigma_y^{(1,1)}$ for the allowed tilt combinations. Interestingly, for $\mathbf{t} = (t_x, 0, t_z)$, we find that the IPHE response is nonzero even when $\theta = \pi/2$, namely the *chiral anomaly* disappears, indicating that the Berry curvature plays a more fundamental role than the *chiral anomaly*. The calculation for the second term $f \sigma_y^{(1,1)}$ is relegated to Supplemental Material³⁵, in which a similar tilt behavior and angular dependence is found. In addition, we note that $\sigma_y^{(1,1)}$ is immune to the choice of C_χ .

At the EB^2 order, we find that only the chirality-dependent term of both ϵ^{BB} and Ω_z^B can lead to a nonvanishing IPHE response. By taking $C_\chi = \chi$ in Eq.(5), the dependence of $\sigma_y^{(1,2)}$ on tilt direction and the θ , contributed by the first term in Eq.(13b) can be expressed as³⁵:

$$\begin{aligned} \sigma_y^{(1,2)} &= \hat{t}_z [C_1 + \hat{t}_x C_2 \sin^2 \theta + \hat{t}_y C_3 \cos^2 \theta] \\ &+ \hat{t}_x \hat{t}_y \hat{t}_z C_4 \sin(2\theta) \end{aligned} \quad (15)$$

Unlike $\sigma_y^{(1,1)}$, a tilt along z -direction is sufficient to achieve

an angular-independent IPHE response. In addition, by applying a further tilt along k_x and/or k_y , we find that the IPHE response will display the angular dependence of $\cos^2 \theta$ and/or $\sin^2 \theta$, as shown in FIG.(1b). At the order of EB^2 , we can identify the more fundamental role of Berry curvature just by exerting a tilt along z -direction when $\mathbf{E} \cdot \mathbf{B} = 0$. The $\sigma_y^{(1,2)}$ contributed by the second term of Eq.(13b), shows slightly different behavior by missing the $\hat{t}_x \hat{t}_z / \hat{t}_y \hat{t}_z$ combinations³⁵.

Finally, at the nonlinear order of $E^2 B^2$, we note that $\sigma_y^{(2,2)}$ is also immune to the choice of C_χ . Focusing on $\sigma_y^{(2,2)}$ contributed by the first term of Eq.(13c), by taking $C_\chi = \chi$ we find³⁵

$$\sigma_y^{(2,2)} = \hat{t}_x C_1 \sin(2\theta) + \hat{t}_y C_2 \sin^2 \theta, \quad (16)$$

Different from the EB and EB^2 orders, we find that the tilt along the z direction is no longer a necessary condition to observe a nonzero IPHE response. The dependence on tilt direction and the θ for $\sigma_y^{(2,2)}$ is shown in FIG.(1c), from which we find that a tilt along y direction will manifest the fundamental role of Berry curvature at $\theta = \pi/2$. The remaining terms of $\sigma_y^{(2,2)}$ are discussed in Supplemental Material³⁵, in which the second term shows the most complex dependence on the tilt and θ and the last term shows a similar dependence on tilt but a slightly different angular dependence. Note that in this work, we only consider the linearly tilted WSMs, if the WSMs allow quadratic tilt, an extra dependence on tilt direction and the θ to achieve the IPHE response may also be found in different orders.

Finally, we confirm that the extrinsic PHE response can also emerge when the *chiral anomaly* is missing within the semiclassical theory. Particularly, by solving the Boltzmann equation armed with the Eq. (1), the dependence on tilt direction and θ for the extrinsic PHE conductivity tensor at the order of EB^2 is found³⁵:

$$\sigma_{\tau,y}^{(1,2)} = C_1 \sin(2\theta) + \hat{t}_x \hat{t}_y [C_2 \cos(2\theta) + C_3] \quad (17)$$

where the first term has been obtained just by considering the first-order semiclassical theory³⁰, which doesn't depend on the tilt direction. With the correction from the second order semiclassical theory, we acquire an extra contribution, $C_2 \cos(2\theta) + C_3$, as shown in FIG.(1d), which also appears in the IPHE in the same order but features different tilt directions. Interestingly, we find that the extrinsic PHE response is also nonvanishing when $\theta = \pi/2$ when \mathbf{t} has a nonzero projection on t_x - t_y plane, indicating the more fundamental role of the Berry curvature, consistent with the IPHE response.

Strategy to detect the IPHE — To detect an IPHE response, we find the tilt of WSMs is the key, following our previous discussion. The relation between the tilt vector and the device is illustrated in FIG.(2), in which the tilt vector is usually along the principal axis of the crystal⁴⁸. Importantly, a single tilt t_α with $\alpha = x, y, z$ can ensure the realization of the IPHE response at the order of EB^2 or $E^2 B^2$. Following the experimental progress of magnetic WSMs, we find that the recent reported magnetic WSM $\text{Co}_3\text{Sn}_2\text{S}_2$ ⁴⁹ with tilted

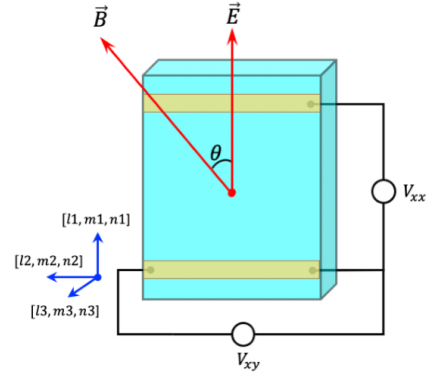


FIG. 2. The schematic device to detect IPHE experimentally. Here $\hat{\mathbf{E}} = \hat{e}_x$, $\hat{\mathbf{B}} = \cos \theta \hat{e}_x + \sin \theta \hat{e}_y$, and $[l, m, n]$ is the Miller index which can be along the principal axis of the crystal so that \mathbf{t} can have a nonzero t_α -component.

Weyl nodes may offer a suitable platform to achieve IPHE response. We comment that the background IAHE response in magnetic WSMs can be easily removed from the detected IPHE response by tuning the magnitude of \mathbf{B} -field (IAHE is free of \mathbf{B}) or the angle θ formed by \mathbf{E} and \mathbf{B} .

In addition, when performing experiment measurement, both the intrinsic and extrinsic PHE responses exist and hence how distinguish them is also important. Although the different dependence on tilt direction and the θ formed by \mathbf{E} and \mathbf{B} offers a tempting approach to isolating IPHE from extrinsic PHE, using the anti-symmetric property of the IPHE conductivity tensor is more favorable experimentally. For instance, when the \mathbf{t} and \mathbf{B} is fixed, one can measure two Hall voltages at $\theta = 0$ and $\theta = \pi/2$ by steering the \mathbf{E} to isolate IPHE response by $\sigma^{\text{anti}} = (\sigma_y^{(l,m)} - \sigma_x^{(l,m)})/2$. And the angular dependence on the fixed tilt direction (if we know) can also be used to double-check this isolation.

Conclusion — In summary, armed with the semiclassical theory up to the second order, we predict that the IPHE can appear in \mathcal{T} -broken WSMs. We unveil that the IPHE is engendered by the (field-induced) Berry curvature with the consideration of energy correction for Bloch bands. Using the linearly tilted effective model, the dependence of IPHE conductivity tensor on the tilt direction and the angle formed by \mathbf{E} and \mathbf{B} are discussed. Interestingly, by studying the angular dependence of the IPHE conductivity tensor, we find that the IPHE response exists even when $\mathbf{E} \cdot \mathbf{B} = 0$, indicating that the Berry curvature plays a more fundamental role than the *chiral anomaly* in WSMs. Finally, the experimental strategy to distinguish the IPHE response from the IAHE and the extrinsic PHE responses of the magnetic WSMs are discussed, by using the anti-symmetric property of the IPHE conductivity tensor. Our work offers a novel intrinsic topological response function to detect \mathcal{T} -broken WSMs and may facilitate the understanding of the experimental measurements performed in the magnetic WSMs.

Acknowledgments — We thank Dr. L.Y. Wang for helpful discussions. This work was supported by the National Natural

Science Foundation of China (Grant Nos. 12034014).

-
- * jianwang@hku.hk
- ¹ X.-G. Wen, Quantum Field Theory of Many-Body Systems (Oxford University Press, New York, 2004).
 - ² K. v. Klitzing, G. Dorda, and M. Pepper, Phys. Rev. Lett. 45, 494, (1980).
 - ³ D. J. Thouless, M. Kohmoto, M. P. Nightingale, and M. den Nijs, Phys. Rev. Lett. 49, 405, (1982).
 - ⁴ F. D. M. Haldane, Phys. Rev. Lett. 61, 2015, (1988).
 - ⁵ C. L. Kane and E. J. Mele, Phys. Rev. Lett. 95, 226801, (2005).
 - ⁶ B. A. Bernevig, T. L. Hughes, and S.-C. Zhang, Science 314 (5806), 1757, (2006).
 - ⁷ H.-J. Zhang, C.-X. Liu, X.-L. Qi, X. Dai, Z. Fang, and S.-C. Zhang, Nature Physics 5 (6), 438, (2009).
 - ⁸ M. König, S. Wiedmann, C. Brune, A. Roth, H. Buhmann, L. W. Molenkamp, X.-L. Qi, and S.-C. Zhang, Science 318 (5851), 766, (2017).
 - ⁹ Y.L. Chen, J. G. Analytis, J.-H. Chu, Z.K. Liu, S.-K. Mo, X.-L. Qi, H.J. Zhang, D.H. Lu, X. Dai, Z. Fang, S.-C. Zhang, I. R. Fisher, Z. Hussain, and Z.X. Shen, Science 325 (5937), 178, (2009).
 - ¹⁰ C.-Z. Chang, J.S. Zhang, X. Feng, J. Shen, Z.-C. Zhang, M.H. Guo, K. Li, Y.B. Ou, P. Wei, L.-L. Wang, Z.-Q. Ji, Y. Feng, S.H. Ji, X. Chen, J.F. Jia, X. Dai, Z. Fang, S.-C. Zhang, K. He, Y.Y. Wang, L. Lu, X.-C. Ma, and Q.-K. Xue, Science 340 (6129), 167, (2013).
 - ¹¹ T. T. Zhang, Y. Jiang, Z.D. Song, H. Huang, Y.Q. He, Z. Fang, H. M. Weng, and C. Fang, Nature 566, 475 (2019).
 - ¹² M.G. Vergniory, L. Elcoro, C. Felser, N. Regnault, B. A. Bernevig, and Z.J. Wang, Nature 566 (7745), 480, (2019).
 - ¹³ F. Tang, H. C. Po, A. Vishwanath, and X.G. Wan, Nature 566 (7745), 486, (2019).
 - ¹⁴ Z.J. Wang, Y. Sun, X.-Q. Chen, C. Franchini, G. Xu, H.M. Weng, X. Dai, and Z. Fang Phys. Rev. B 85, 195320, (2012).
 - ¹⁵ Z.K. Liu, B. Zhou, Y. Zhang, Z.J. Wang, H.M. Weng, D. Prabhakaran, S.-K. Mo, Z.X. Shen, Z. Fang, X. Dai, Z. Hussain, and YL Chen, Science 343 (6173), 864, (2014).
 - ¹⁶ X. Wan, A. M. Turner, A. Vishwanath, and S. Y. Savrasov, Phys. Rev. B 83, 205101 (2011).
 - ¹⁷ H.M. Weng, C. Fang, Z. Fang, B. A. Bernevig, and X. Dai, Phys. Rev. X 5, 011029, (2015).
 - ¹⁸ S.-M. Huang, S.-Y. Xu, I. Belopolski, C.-C. Lee, G. Chang, B.K. Wang, N. Alidoust, G. Bian, M. Neupane, C. Zhang, S. Jia, A. Bansil, H. Lin, and M. Z. Hasan, Nature Communications 6, 7373, (2015).
 - ¹⁹ N. P. Armitage, E. J. Mele, and A. Vishwanath, Rev. Mod. Phys. 90, 015001 (2016).
 - ²⁰ S.K. Das, T. Nag, and S. Nandy, Phys. Rev. B 104, 115420 (2021).
 - ²¹ Q. Li, D. E. Kharzeev, C. Zhang, Y. Huang, I. Pletikosić, A. V. Fedorov, R. D. Zhong, J. A. Schneeloch, G. D. Gu, and T. Valla, Nature Physics. 12, 550 (2016).
 - ²² C. Z. Li, L. X. Wang, H. W. Liu, J. Wang, Z. M. Liao, and D. P. Yu, Nat. Commun. 6, 10137 (2015).
 - ²³ C. L. Zhang et al, Nat. Commun. 7, 10735 (2016).
 - ²⁴ X.H. Huang, L.X. Zhao, Y.J. Long, P.P. Wang, D. Chen, Z.H. Yang, H. Liang, M.Q. Xue, H.M. Weng, Z. Fang, X. Dai, and G.F. Chen, Phys. Rev. X 5, 031023 (2015).
 - ²⁵ S. Adler, Phys. Rev. 177, 2426 (1969).
 - ²⁶ J. S. Bell and R. Jackiw, Nuovo Cimento A 60, 47 (1969).
 - ²⁷ D. T. Son and B. Z. Spivak, Phys. Rev. B 88, 104412 (2013).
 - ²⁸ K. S. Kim, H. J. Kim, and M. Sasaki, Phys. Rev. B 89, 195137 (2014).
 - ²⁹ A. A. Burkov, Phys. Rev. Lett. 113, 247203 (2014).
 - ³⁰ S. Nandy, Girish Sharma, A. Taraphder, and Sumanta Tewari, Phys. Rev. Lett. 119, 176804 (2017).
 - ³¹ A. A. Soluyanov, D. Gresch, Z. J. Wang, Q. S. Wu, M. Troyer, X. Dai, and B. A. Bernevig, Nature (London) 527, 495 (2015).
 - ³² D. Xiao, M.-C. Chang, and Q. Niu, Rev. Mod. Phys. 82, 1959 (2010).
 - ³³ Y. Gao, S.Y.A. Yang, and Q. Niu, Phys. Rev. Lett. 112, 166601 (2014).
 - ³⁴ For simplicity, we have suppressed the band index of f_k , Berry curvature $\tilde{\Omega}_z$, and band energy.
 - ³⁵ Supplemental material.
 - ³⁶ V. A. Zyuzin, Phys. Rev. B 95, 245128 (2017).
 - ³⁷ Y. Ferreira, A. A. Zyuzin, and J. H. Bardarson, Phys. Rev. B 96, 115202 (2017).
 - ³⁸ S. K. Das, T. Nag, and S. Nandy, Phys. Rev. B 104, 115420 (2021).
 - ³⁹ Y. J. Wu, H.W. Liu, H. Jiang, and X. C. Xie, Phys. Rev. B 96, 024201 (2017).
 - ⁴⁰ D. Ma, H. Jiang, H.W. Liu, and X. C. Xie, Phys. Rev. B 99, 115121 (2019).
 - ⁴¹ G. Sharma, P. Goswami, and S. Tewari, Phys. Rev. B 96, 045112 (2017).
 - ⁴² T. M. McCormick, R. C. McKay, and N. Trivedi, Phys. Rev. B 96, 235116 (2017).
 - ⁴³ F. Y. Li, X. Luo, X. Dai, Y. Yu, F. Zhang, and G. Chen, Phys. Rev. B 94, 121105(R) (2016).
 - ⁴⁴ H. Z. Lu, S. Q. Shen, Front. Phys. 12, 127201 (2017).
 - ⁴⁵ M. A. Stephanov and Y. Yin, Phys. Rev. Lett. 109, 162001 (2012).
 - ⁴⁶ D. T. Son and N. Yamamoto, Phys. Rev. Lett. 109, 181602 (2012).
 - ⁴⁷ The f' of the first term of $W^{(1,1)}$ can be obtained by performing integration by parts.
 - ⁴⁸ For instance, the first-principles calculation shows that the Weyl cone is tilted along b -axis for WTe_2 ^{31,50}.
 - ⁴⁹ E.K. Liu, Y. Sun, N. Kumar, L. Muechler, A. Sun, L. Jiao, S.-Y. Yang, D. Liu, A. Liang, Q. Xu, J. Kroder, V. Süß, H. Borrmann, C. Shekhar, Z.S. Wang, C.Y. Xi, W.H. Wang, W. Schnelle, S. Wirth, Y.L. Chen, S. T. B. Goennenwein and C. Felser, Nature Physics 14 (11), 1125, (2018).
 - ⁵⁰ C. Wang et al., Phys. Rev. B 94, 241119(R) (2016).